Weighted-Average Isostrain and Isostress Model to Describe the Kinetic Evolution of the Mechanical Properties of a Composite Gel: Application to the System Gelatin:Maltodextrin

VALÉRY NORMAND, PAUL D. A. PUDNEY, PIERRE AYMARD, IAN T. NORTON

Unilever Research, Colworth, Sharnbrook, Bedford MK44 1LQ, United Kingdom

Received 14 September 1999; accepted 8 November 1999

ABSTRACT: Application of a weighted-average model (WAM) to the kinetic evolution of the elasticity during 16 h was successfully performed for a composite gel in which a maltodextrin phase is dispersed within a continuous gelatin phase. The results obtained using the model for different starting compositions along an initial higher-temperature binodal are in good agreement with the phase diagram measured at high temperature and help to confirm the position of the binodal. A novel application of confocal Raman microscopy was used to measure the local concentration of the included phase of the composite gel and confirms the results given by the WAM. This model allows calculation of tie lines appropriate to the gel state and could be used for other biopolymer blends if the assumption is made that the gelation process involves a complete phase separation of both polymers before any gelation occurs. © 2000 John Wiley & Sons, Inc. J Appl Polym Sci 77: 1465–1477, 2000

Key words: phase separation; master curve; small deformations; confocal Raman spectroscopy

INTRODUCTION

The prediction of the mechanical properties of a blended biopolymer gel is of interest to the food industry (e.g., relevant to low-fat spreads and ice cream). This is a difficult problem whose study has been pioneered in the past mainly for blended synthetic polymer systems.[1,2] For composite biopolymer gels, the Takayanagi model suggested by this earlier work was used in its simplest form to describe the equilibrium modulus in terms of component concentrations within phases and volume fractions of these phases (upper- and lower-bound model).[3–7] However, Takayanagi introduced a more complex model for polymer-blend systems in the situation where one polymer is discontinuously dispersed in a matrix of the other. This model involves a nonuniform distribution of stress and strain in the sample and was tested on films based on a styrene–acrylonitrile copolymer and nitrile–butadiene rubber. The most important conclusion reached was that the shape of the inclusions, or the anisotropy of distribution of these inclusions, could be deduced from two parameters of the model linked to the phase volume of the included phase. This model can also describe the filler effect even when the moduli of the two phases are of the same order of magnitude.

In other fields of research, models of this kind have also been extensively developed. For exam-

Correspondence to: V. Normand.

Contract grant sponsor: Commission of the European Communities, Agriculture and Fisheries (FAIR); contract grant number: CT 1015.

Journal of Applied Polymer Science, Vol. 77, 1465–1477 (2000)

ple, in conductivity, where the resistance of a cocontinuous composite material was analytically formulated,[8] in polymer blend systems,[9] in 3-D textile composites where the weight-average model (WAM) was suggested for the first time,[10] and in biomedical research where fibers have been used as reinforcements in composites.[11] This last approach was numerical and involved composites made from fibers embedded in a polymer matrix. The model consists of averaging the local contributions of stress and strain when the sample is loaded under different conditions.

The gelatin:maltodextrin system considered here has already been extensively described by Kasapis et al.[12–15] However, in all of the rheological analyses performed, these authors dealt with the change in the equilibrium modulus (i.e., modulus at long time) when maltodextrin was added at a constant gelatin concentration. The purpose of the present study was to investigate the rheological behavior of systems where the component biopolymers initially form two separate phases, in thermodynamic equilibrium, and where one phase remains dispersed in the other. A predictive model for the kinetic evolution of the composite gel elastic modulus was then developed.

To confirm the predictions of this model, the concentration of the component within the included phase of the biopolymer composite needs to be known. Durrani et al.[16–18] developed a method which gives access to the local concentrations of biopolymer mixtures using Fourier transform infrared spectroscopy. However, this technique is applicable only to large particle sizes as the spatial resolution is limited in infrared microscopy by the infrared wavelength, which, at best, gives an approximately 20-micron spatial resolution (40 microns was suggested by Durrani et al.[18]). The other major limitation is that, because the infrared beam goes through the entire sample, the technique cannot be made confocal. This means that particles have to be large enough to fill the whole gap between the slides, and even if this is the case (in practice, very few systems will have particles that large), it is very difficult to prevent the matrix phase from being trapped between the particles and the slide, which also leads to erroneous results. In the present study, the local concentration of the inclusions was measured directly *in situ* in the matrix, for the first time, using Raman spectroscopy. This method gives better spatial resolution, due both to the wavelength of the light and the fact that Raman spectroscopy can exploit the confocal effect and, thus, can spatially resolve in 3D, rather than just 2D. The instrument used in the present study had a spatial resolution of 2 μm, which allows particles of approximately 4–5-μm diameter to have their concentration measured accurately *in situ*. The full details of this method were reported elsewhere,[19] with only relevant results being shown here and compared to the proposed model. Here, most of the study deals with system compositions located on the initial high-temperature binodal.

EXPERIMENTAL

Lime hide gelatin (LH1e) was provided by SKW Biosystem (Carentan, France) and maltodextrin Paselli (SA2) by AVEBE (Ulceby, UK). The gelatin LH1e (PI = 4.7; $\bar{M}_n$ = 83300 D; polydispersity = 1.77, measured by GPC) was a polypeptidic biopolymer obtained after alkaline degradation of collagen and the maltodextrin, a polysaccharide obtained by enzymatic degradation of potato starch[20] ($\bar{M}_n$ = 6.2 ± 0.5 10^5 D; polydispersity = 1.45 ± 0.30, measured by light scattering).

Mixtures of these two biopolymers at 60°C show an important incompatible domain at high concentrations (Fig. 1). However, at low concentrations, a compatible domain exists. These two domains are separated by the binodal curve.

Both biopolymer solutions were prepared separately at a 0.1*M* ionic strength before being mixed. NaCl was added, taking into account the salt content of the biopolymer powders. To ensure that the composition chosen for the cure experiments belonged exactly to the binodal at 60°C, initially incompatible systems were considered, an appropriate mixture of the two biopolymer solutions being held quiescently at 60°C for 4 h. This allowed the system to equilibrate into two separated phases. The gelatin-rich phase creams while the maltodextrin-rich phase sediments.

Both phases, the top phase (gelatin-rich phase) and the bottom phase (maltodextrin-rich phase) were then isolated and cooled at 1°C/min from 60 to 11°C in both simple gap coaxial cylinders at a large gap[21] and a parallel-plate system (1-mm gap) and maintained at 11°C for 16 h. The elasticity (G') was measured at 1 Hz and 0.5% strain with a Carrimed CSL 500 to follow the gel formation. All samples were measured within their linear viscoelastic region. The starting compositions are plotted in Figure 1:

System I: 4% LH1e, 10% SA2, 0.1*M* NaCl.

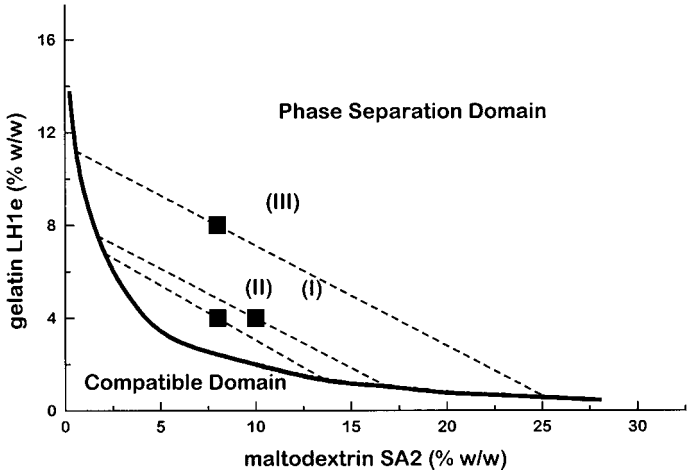

Figure 1 Phase diagram of the system LH1e:SA2:0.1*M* NaCl, measured at 60°C. Systems I, II, and III are, respectively, 4% LH1e:10% SA2, 4% LH1e:8% SA2, and 8% LH1e:8% SA2. Tie lines according to volumes are plotted by dashed lines.

System II: 4% LH1e, 8% SA2, 0.1*M* NaCl.
System III: 8% LH1e, 8% SA2, 0.1*M* NaCl.

When confocal scanning laser microscopy was applied, the gelatin was stained using 500 ppm of Sirius Red to increase the fluorescence contrast between the two biopolymers. However, when confocal Raman spectroscopy was employed, the autofluorescence of the gelatin generated sufficient contrast prior to measurement.

In recent years, Raman spectrometers have advanced greatly and now allow weak Raman scattering systems to be studied that were previously inaccessible. They also allow their study in a confocal manner.[22] In addition, reliable lasers have become available in the NIR region which allow systems, which would normally be dominated by fluorescence, such as biopolymers, to be studied. A confocal Raman spectrometer (Renishaw plc, Gloucestershire, UK) was coupled to an Olympus BH2 micro-

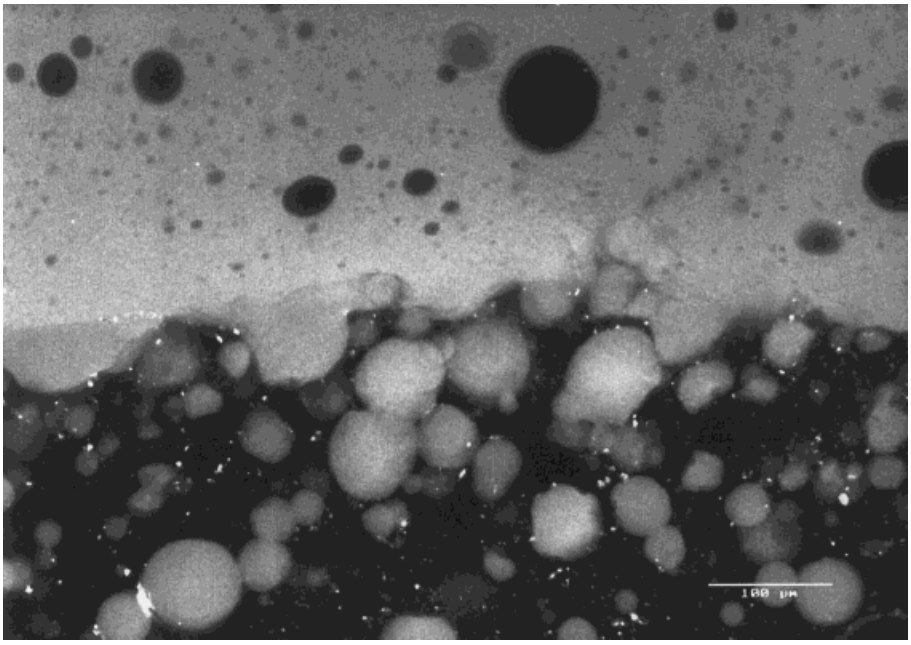

Figure 2 System I cooled from 60 to 11°C at 1°C/min; structure at the phase junction (gelatin is bright, maltodextrin is dark).

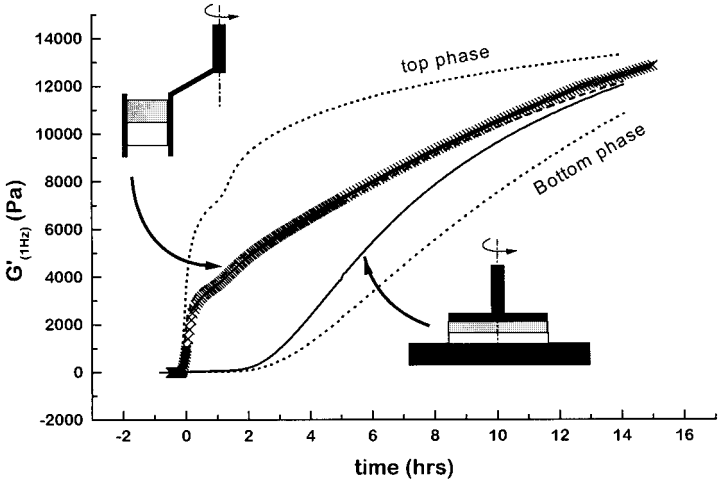

Figure 3 Bulk-phase separation of system I: (×) comparison between coaxial cylinders and (–) calculated value from eq. (1) according to the phase volumes. (—) The calculated value according to eq. (2) corresponds to the measurement between parallel plates. The elasticity of the top and bottom phases is shown by the dotted lines.

scope with a motorized XYZ stage, using a 782-nm diode laser as the excitation source. All spectra shown in this work were taken with a 50× microscope objective, which gives a focal spot of approximately 2-μm diameter. All spectra were collected with an exposure time of 60 s, with three accumulations being averaged.

RESULTS

Evidence of Anisotropy in the Bulk-phase-separated System

Starting from a phase-separated state, and applying a cooling rate of 1°C/min from 60 to 11°C, formation of two layers can be distinguished, before gelation of the first layer occurs. The microstructure of the heterogeneous sample is given in Figure 2 where the gelatin appears as bright areas and the maltodextrin is dark. The separation does occur, however, in a simple manner, as gelatin droplet formation can be seen in the maltodextrin phase and maltodextrin inclusions can also be seen in the gelatin-rich phase. On the other hand, when the system is held at 60°C for 4 h, droplets are not present in either phase. This indicates that the top and bottom phases are both compatible mixtures at high temperature and that droplet formation occurs during the cooling process, these being trapped by the gelation of the phase.

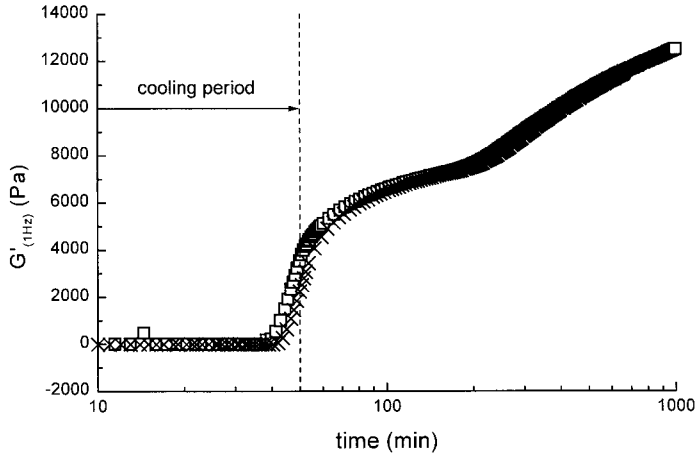

Figure 4 Isotropic behavior found in the top phase of the system I: (□) parallel plates; (×) concentric cylinders at simple gap.

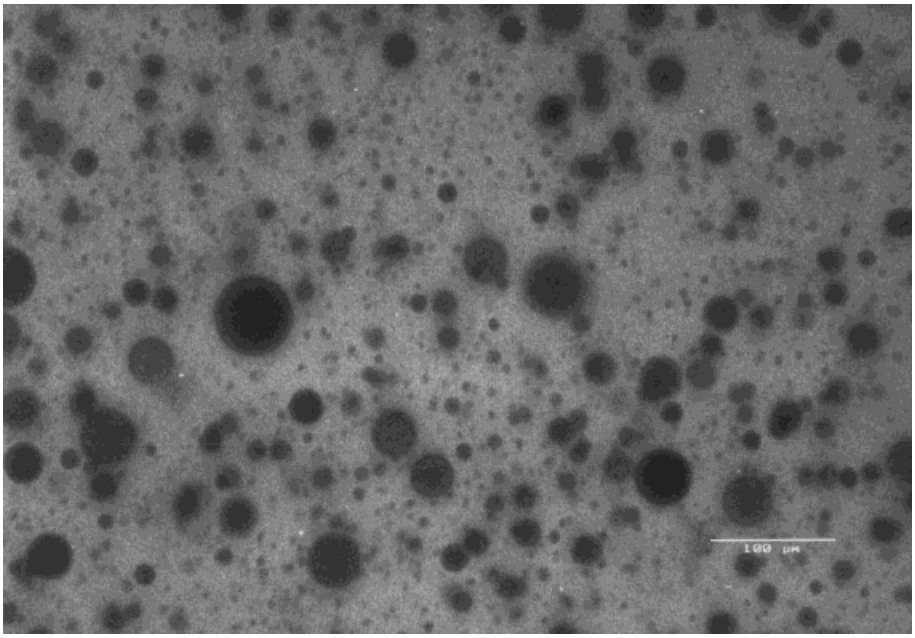

Figure 5 Microstructure of the top phase of system I. System cooled at 1°C/min from 60 to 11°C and cured 16 at 11°C.

A system which phase separates into two layers is anisotropic, and its rheology depends on the measurement geometry. The overall rheological characteristics can then be expressed as linear combinations of the rheologies of the individual layers, each weighted according to layer volume.[1] If the measurements are performed using coaxial cylinders, the isostrain relationship (upper bound) is appropriate:

$$hG'_c = h_1G'_1 + h_2G'_2 \tag{1}$$

while if parallel plates are used, the isostress relationship (lower bound) should be applied:

$$\frac{h}{G'_c} = \frac{h_1}{G'_1} + \frac{h_2}{G'_2} \tag{2}$$

Here, h is the total height of the sample; h_1 and h_2, the heights of both layers; and G'_c, G'_1 , and G'_2, respectively, the modulus of the composite and the modulus of either layer.

The experimental modulus of system I and the moduli of the separate individual phases were measured between coaxial cylinders, following the same thermal history as that of the layered system. The phase-volume fractions were evaluated as 0.46 for the top phase and 0.54 for the bottom phase. The results are plotted in Figure 3, where the elasticity of system I is directly compared to the predictions of both the upper- and lower-bound models. Corresponding data are not available for the parallel-plate experiment as it appears that a 1-mm gap is not large enough to avoid surface interactions due to the plates, which affect the separation into two layers. As shown in Figure 3, good agreement is obtained when the upper-bound relationship is compared to the results of measurement performed between coaxial cylinders. Interestingly, the results of the upper- and lower-bound models lead to the same modulus value at long times (after 14 h at 11°C). However, the early stage of gelation shows differences. Since the separation of the layers occurs according to the phase diagram (Fig. 1), each individual layer has a composition located on the binodal. Hence, both biopolymers are present in each phase and two gelation events are expected. This is clearly seen in Figure 3 for the top phase. An advantage of studying this top phase is that gelation of the inclusions happens after gelation of the continuous phase. However, for the bottom phase, the gelatin forms the inclusions and gels before the maltodextrin. In this situation, the modulus only starts to increase when an infinite maltodextrin gel appears, and this is affected in an unpredictable way from the early stage of the gelation by the presence of the gelatin inclusions.

Thus, in the present article, only the top phase will be examined further.

Characterization of the Top Phase

The real composition of the top-phase sample and the corresponding tie-line directions can be roughly estimated by the phase-volume method, effective when the binodal line is well defined. The most important information available is that, at 60°C, the system corresponds to a point on the binodal in the gelatin-rich part of the phase diagram.

The evolution of the elasticity shows two well-defined steps with time, as shown in Figure 3, where the elapsed time was chosen to start at the end of the cooling stage. The two steps in the gel-strength evolution are related to the gelation of separate phases. The first gelation process starts at around −10 min and at a temperature of about 19.5°C, while the second starts after approximately 100 min after the sample reached 11°C. The gelation curve of the top phase is geometry-independent, as shown in Figure 4, and the phase is therefore isotropic.

The microstructure of the gelled top phase of system I is shown in Figure 5, where the maltodextrin-included phase is dark and the continuous gelatin phase is light. This micrograph reveals a continuous gelatin phase and a maltodextrin phase confined to small droplets. These droplets do not percolate to form a network through the sample. The shape of the droplets appears uniform and spherical. However, the size of the droplets is very heterogeneous and varies from 1 to more than 50 microns in diameter. According to microscopy work performed in the compatible domain of the phase diagram, formation of maltodextrin droplets precedes gelation of the gelatin, and the demixing process occurs when the sample is in the liquid state.

Model Description

A first assumption made was that the gelatin-rich mixture located on the binodal separates on cooling into two phases containing the pure individual biopolymers (i.e., the new tie line extends to the composition axes). For such a situation, the upper- and lower-bound models of Takayanagi were used by several authors to describe long-time values of the elasticity moduli (G') of gelatin and maltodextrin mixtures.[6,15] Unfortunately, these models fail significantly when the whole gelling curve is considered, that is, from the sol state to the fully cured gel state.

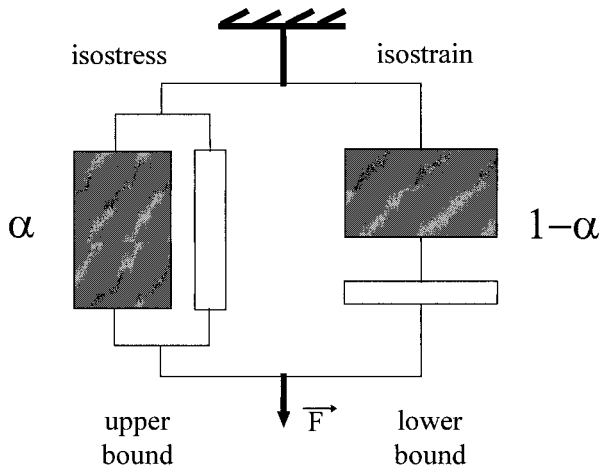

Figure 6 Schematic representation of the combined model. The continuous phase is shaded and the included phase is white. The force applied is denoted F.

According to McEvoy et al.,[4] a solution containing two polymers which phase separate into two pure polymer phases during gelation responds according to a lower-bound model if the included phase is stronger than the continuous phase and according to an upper-bound model if the included phase is the weakest phase. Strain and stress distributions are the important field variables in these two models, and uniform distributions for at least one of the fields is assumed in each limit. In the case of gelation of the gelatin:maltodextrin mixture studied here, the strengths of the individual gel phases increase with time, and the ratio of strengths can be inverted during cure, depending of the kinetics of gelation of each of the individual components.

The model proposed here to completely describe the behavior of such a system during cure is a combination of the upper- and lower-bound models as indicated in Figure 6 using the schematic model of series and parallel elements. As a consequence of these assumptions, we can model the behavior of the elastic response, which depends on the arrangement of the included phase in relationship to the direction of the applied force. If the proportion of the isostrain component included in the model is called "α" and the isostress part "$1 - \alpha$," the equation for the composite modulus associated with this model takes the following form:

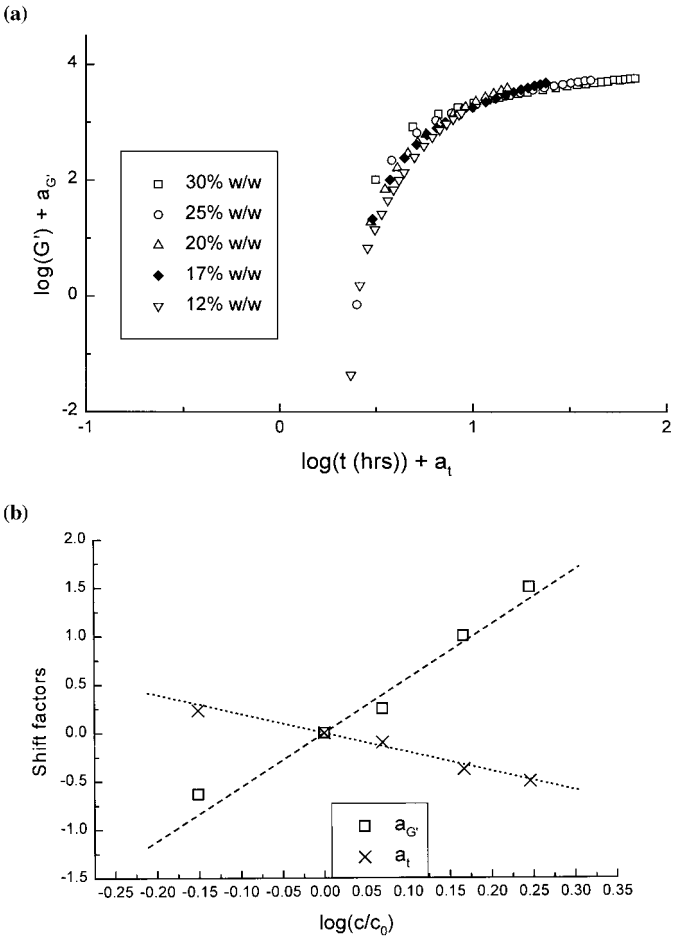

Figure 7 (a) Master curve for maltodextrin SA2 measured at 11°C after a cooling rate from 60 to 11°C at 1°C/min. (b) Determination of the exponents related to the concentration for maltodextrin SA2.

$$G'_c(t) = \alpha[(1-\phi)G'_{LH1}(t) + \phi G'_{SA2}(t)] + (1-\alpha) \times \left[\frac{1-\phi}{G'_{LH1}(t)} + \frac{\phi}{G'_{SA2}(t)}\right]^{-1} \quad (3)$$

where $G'_c(t)$ represents the kinetic evolution of the elastic modulus of the composite gel; α, the isostrain fraction; ϕ, the volume fraction of the SA2-included phase; and $G'_{LH1}(t)$ and $G'_{SA2}(t)$, the kinetic evolutions of the elastic moduli of the gelatin and of the maltodextrin phases, respectively, at given local concentrations.

In the present case, the composition of the starting phase is not accurately known, but when cure curves for the individual biopolymers are available for given concentrations, it becomes possible to simulate the kinetics of gelation of the composite using a computer model. Over certain concentration ranges, the modulus of a gelatin gel is known to be dependent on the square of its concentration[23]:

$$G'_1 = \left(\frac{c_1}{c_0}\right)^{2.0} G'_0 \quad (4)$$

where G'_1 represents the equilibrium elastic modulus for a concentration c_1, and G'_0, the reference equilibrium elastic modulus at the reference concentration c_0.

Master Curve for Gelatin Gelation

It was recently shown that the κ-carrageenan gel modulus can be estimated at any time and for any concentration between 0.01 and 0.2% w/w in 0.01*M* KCl, as a gelation master curve can be deduced by shifting horizontally and vertically

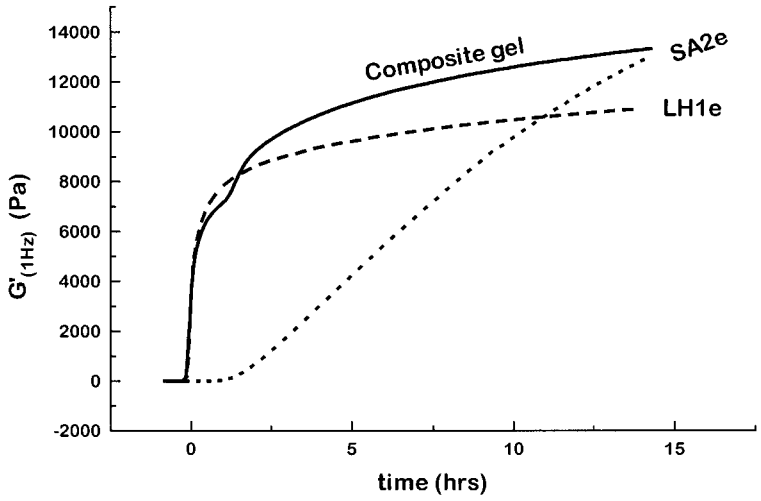

Figure 8 Gelation profiles for the top phase of system I, gelatin LH1e at 8% w/w and maltodextrin SA2 17% w/w in 0.1*M* NaCl, and between concentric cylinders.

the individual cure curves in a bilogarithmic representation.[24] The same empirical exercise was attempted on a lime hide gelatin identical to the one studied here[25] and results are shown below:

$$G'_1(t) = \left(\frac{[\text{LH1e}]_1}{[\text{LH1e}]_0}\right)^{2.0\pm0.2} G'_0(t) \qquad 3\% \le [\text{LH1e}] \le 10\% \text{ w/w} \quad (5a)$$

This first relationship implied dependence for the gelatin gel modulus similar to that predicted by the cascade model over the same concentration range.[23]

In addition, for the cooling regime applied, the time scale of the gelatin can be described as a function of its reference concentration according to the following relationship:

$$t_1 = \left(\frac{[\text{LH1e}]_1}{[\text{LH1e}]_0}\right)^{-0.9\pm0.18} t_0 \qquad 3\% \le [\text{LH1e}] \le 10\% \text{ w/w} \quad (5b)$$

where t_1 and t_0 are the time scales for the gelatin at the local concentration (1) and reference concentration (0), respectively.

Master Curve for Maltodextrin Gelation

When the same exercise was attempted for maltodextrin gelation curves, using the 17% w/w con-

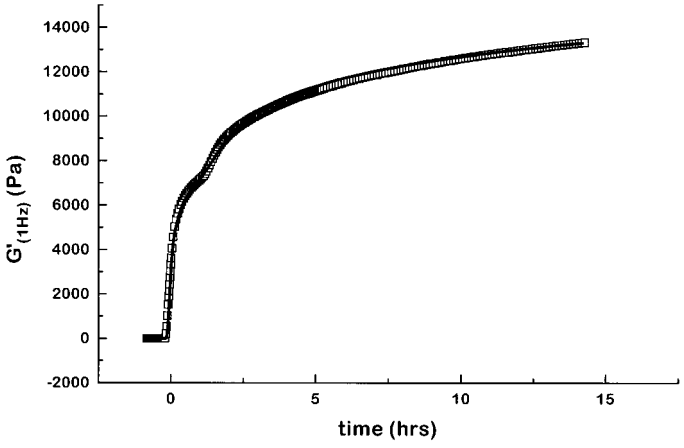

Figure 9 Comparison between experimental data and the best fit according to eq. (3) for the top phase of system I.

Table I Parameters of the Fit for the Three Different Top Phases Using Different Conditions of Measurement (Parallel Plates and Concentric Cylinders)

Parameters	System I LH1e 4% : SA2 10%	System II LH1e 4% : SA2 8%	System III LH1e 8% : SA2 8%
α	0.81 ± 0.04	0.81 ± 0.04	0.93 ± 0.05
ϕ (%)	7.45 ± 1.0	23.85 ± 2.0	1.42 ± 0.55
[LH1e] (% w/w)	8.96 ± 0.28	7.37 ± 0.25	12.54 ± 0.12
[SA2] (% w/w)	16.0 ± 1.18	10.72 ± 1.1	22.48 ± 1.1

The α parameter, the phase volume of the included phase (maltodextrin) and the local concentrations of gelatin and maltodextrin are given.

centration results as a reference, a good, but not perfect, agreement was found in the range 12–30% w/w [Fig. 7(a)]. Two exponents were calculated from the slopes of the shift factors as functions of the logarithms of the concentrations referred to a standard c_0 [Fig. 7(b)]. The values of these exponents allow satisfactory estimation of gelation curves for unmeasured concentrations:

$$G'_1(t) = \left(\frac{[\mathrm{SA2}]_1}{[\mathrm{SA2}]_0}\right)^{5.6\pm0.18} G'_0(t) \qquad 12\% \le [\mathrm{SA2}] \le 30\%\ \mathrm{w/w} \quad (6a)$$

$$t_1 = \left(\frac{[\mathrm{SA2}]_1}{[\mathrm{SA2}]_0}\right)^{-1.9\pm0.16} t_0 \qquad 12\% \le [\mathrm{SA2}] \le 30\%\ \mathrm{w/w} \quad (6b)$$

Application of the Model

Using the above formulas, the modulus of each biopolymer can be expressed as a function of its local concentration and of time. The parameters of the model for the evolution of the composite gel modulus are then

- α, the fraction of the isostrain bound;
- ϕ, the volume fraction of the maltodextrin;
- [LH1e], the local concentration of the gelatin in the gelatin phase; and
- [SA2], the local concentration of the maltodextrin in the maltodextrin phase.

Four adjustable parameters are involved in eq. (3). However, the two local concentrations are unambiguously estimated according to eqs. (5b) and (6b), independently of the two other parameters. This makes α and ϕ the two major parameters in eq. (3).

To determine the best values for the parameters of this model, gelatin LH1e (8% w/w, 0.1*M* NaCl) and SA2 (17% w/w, 0.1*M* NaCl) gels were also measured in both geometries and in the same conditions of temperature history as were the experimental data for the composite gel. Relevant reference curves are plotted in Figure 8 for the concentric cylinders experiment and compared to the composite gel curve of system I. A computer simulation was performed using the least-squared criterion for determining the best fit. The computer program involved four steps, which were repeated until the best agreement was reached; these are resumed below:

- Estimation of the four parameters.
- Calculation of the two cure curves for gelatin and maltodextrin at their respective local concentrations using eqs. (5) and (6).
- Fit of the three individual curves using a cubic spline method in order to get the same increment for all curves.
- Comparison of the calculated combination with the experimental curve by the least-square criterion.

The best fit according to eq. (3) is shown in Figure 9, where the calculation of the modulus was performed using the reference cure curves of the LH1e 8% w/w and the SA2 17% w/w previously presented. The parameter values obtained are presented in Table I.

Raman Spectroscopy Mapping

To validate the predictions of this model, the top phase of system I was examined by confocal Raman spectroscopy. A typical included SA2-rich particle was examined (approximately 10 μm in

diameter). An XY map was then produced by scanning an area of 18 × 14 μm with a step size of 2 μm. At each spot, a Raman spectrum was scanned over 60 s and repeated three times to get the required signal-to-noise ratio. This was then repeated over the 80 points of the chosen area across the included particle. The data were then examined in two ways to produce maps: The first of these was to use the strong SA2 band at 475 cm^{-1}. As intensity in Raman is directly proportional to concentration, a spatial plot of the intensity of this band shows the distribution of SA2. This map matched well the optical microscope picture of the included particle and showed that the particles are SA2-rich (Fig. 10). The second map was produced from a more sophisticated analysis of the spectra using multivariate curve resolution. This method uses the whole spectrum for the analysis and the full details are described elsewhere,[26] but it is an orthogonal projection multivariate curve-resolution method (OP-MCR). It provides information on the number of chemical species present (already known in this case), and it then produces the spectrum of each of these (see Fig. 11). These spectra match the spectra of the pure components[19] well and they can be used to produce a spatial map (Fig. 10), which matches the previous map from the 475 cm^{-1} but at a higher signal-to-noise ratio. The concentration map can then be fully quantified if a calibration is carried out. In this case, a calibration was performed on SA2, and this was used to give a fully quantified map of the included SA2-rich particle and the surrounding matrix. This showed that the peak concentration in the particle was 20 ± 2% w/w SA2, which is close to the value obtain from the rheological model (16.0 ± 1.2 % w/w).

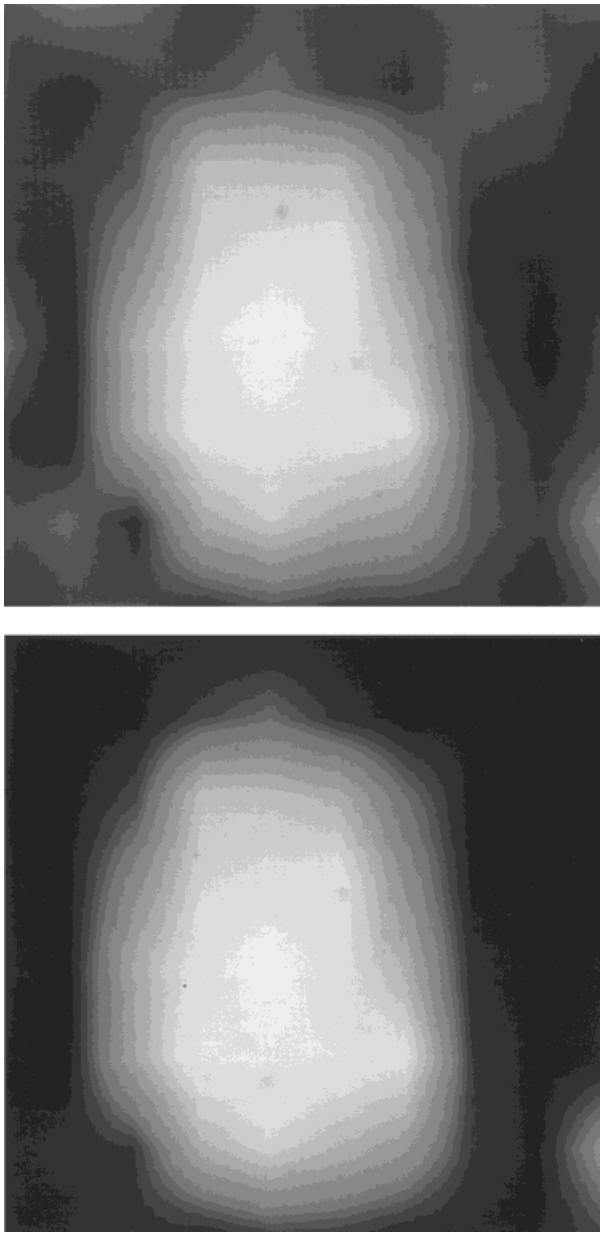

Figure 10 Raman maps of an SA2-included particle in the top phase of system I (a) produced from the SA2 475 cm^{-1} peak and (b) produced from the whole spectrum of MCR factor for the SA2; see Figure 11. Maps dimensions are 18 × 14 μm.

DISCUSSION

The real concentration of both species in the original sample is accessible through a combination of the phase volume and the local concentration of each biopolymer:

$$[\mathrm{LH1e}]_r = (1 - \phi)[\mathrm{LH1e}]_l \quad (7)$$

and

$$[\mathrm{SA2}]_r = (\phi)[\mathrm{SA2}]_l \quad (8)$$

The composition found using eqs. (7) and (8) for the three systems are reported in Table II.

These results are also plotted on the phase diagram for the three systems measured at different experimental conditions in Figure 12. In Figure 12, compositions found using the model are in good agreement with the previous determi-

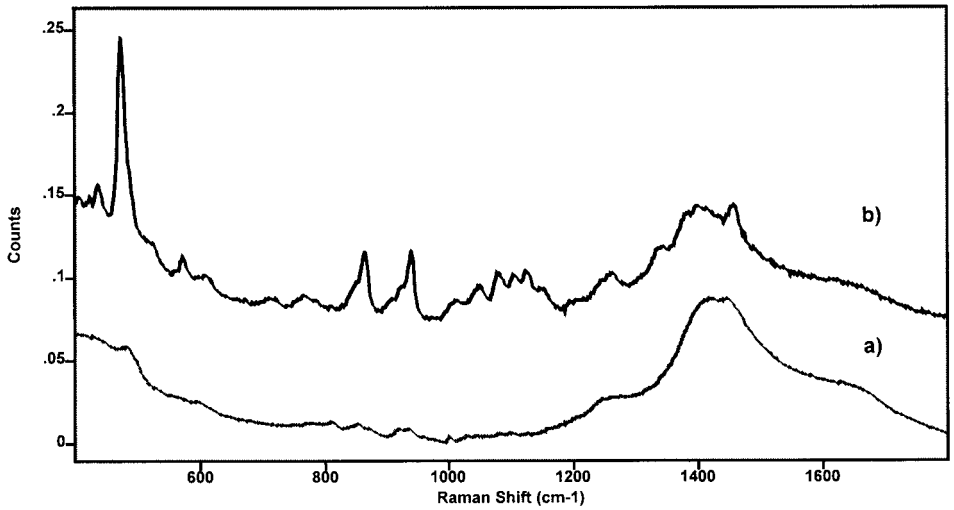

Figure 11 Spectral factors produced from the MCR method (see text) for (a) gelatin and (b) SA2.

nation of the binodal at 60°C. The real concentrations emerging from this model are in good agreement with those obtained by the phase-volume method where the top phase is estimated as containing 7.5% LH1e and 1.7% SA2. Confocal Raman microscopy was used to determine the local concentration of the inclusion and gave results which are consistent with the model used.

As discussed in the work of Kalidindi and Franco,[11] the α parameter was observed to be insensitive to the volume fraction, which is consistent with the way of calculating the fit, as no relationship has been assumed here between α and ϕ. However, it is strongly influenced by the nonaxial properties of the inclusions and then related to the inclusion modulus and these local concentrations.

The tie lines deduced by the model in the gel state are steeper than are the tie lines deduced at 60°C, which suggests that the gelatin becomes more hydrophobic when the temperature decreases. In the Flory–Huggins theory, tie-line slopes are determined by differences of the χ parameters of the individual components in relation to the solvent. An increase in the steepness of the tie line during the gelation process is consistent with an increase in the Flory–Huggins χ parameter of the gelatin from 0.48 to a value close to 0.5 when the temperature decreases.[27] Here, the assumption is made that the χ value for maltodextrin does not change during gelation of the matrix.

CONCLUSIONS

The model of upper and lower bounds used here in the case of gelatin/maltodextrin mixtures is sufficient to explain the rheology of a bulk-phase-separated system, or layered system, as a linear combination of contributions from each separated phase. For a gelled homogeneous upper layer, the rheological model proposed here

Table II Comparison of the Composition of the Top Phases Using Different Experimental Conditions: Phase Volume Method (PVM) at 60°C and WAM in Concentric Cylinders and in Parallel Plates

	System I		System II		System III	
Composition	PVM	Model	PVM	Model	PVM	Model
[LH1e] (% w/w)	7.5	8.30 ± 0.17	6.8	5.61 ± 0.15	11.2	12.36 ± 0.07
[SA2] (% w/w)	1.7	1.20 ± 0.26	2.1	2.54 ± 0.5	0.6	0.2 ± 0.08

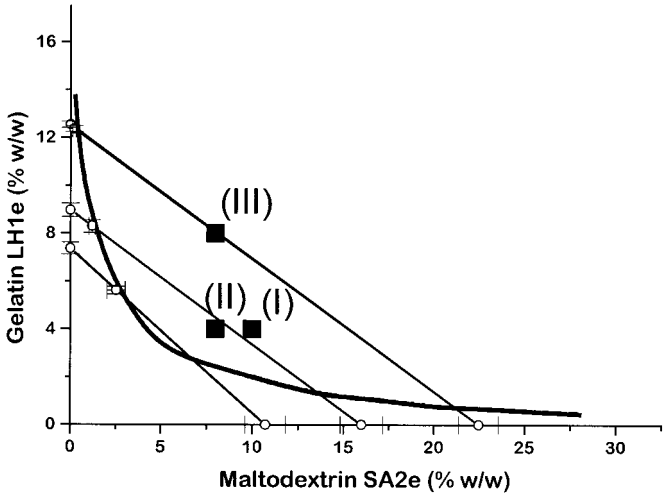

Figure 12 Comparison between the binodal composition of the top phase resulting from the model for the three systems studied.

for the gelatin:maltodextrin mixed system (WAM) assumes complete separation of the components on cooling and a combination of upper- and lower-bound contributions in order to explain the data. By doing this, a phase diagram for the gelled state can be predicted and the move of the binodal with temperature due to gelation of one of the species. The resulting phase diagram showed a great increase in the phase-separated domain and steeper tie lines than those measured at higher temperatures. This result is in accordance with an increase of the hydrophobicity of the gelatin chains during the ordering and gelation process.

The model showed no evidence of anisotropy in the samples, which separated into two phases with one polymer phase-dispersed within a continuous phase of the other. The concentration of such included phases could be measured by a novel application of confocal Raman spectroscopy. A master curve for gelation of maltodextrin was determined which allows satisfactory estimation for the gelation curves at concentrations between 12 and 30% w/w.

This work was carried out with financial support from the Commission of the European Communities, Agriculture and Fisheries (FAIR) specific RTD program, CT 1015, "Mixed Biopolymers: Mechanism and Application of Phase Separation." The authors would like to thank Prof. A. H. Clark for fruitful discussions and comments, Dr. D. Ferdinando for the CSLM measurements, Renishaw plc for the loan of the confocal Raman spectrometer, Dr. T. Hancewicz for help with the MCR analysis of the Raman data, and Mr. S. Mathieu for his experimental work.

REFERENCES

1. Takayanagi, M.; Harima, H.; Iwata, Y. Mem Fac Eng Kyushu Univ 1963, 23, 3–13.
2. Nielsen, L. E. In Mechanical Properties of Polymers Composites; Marcel Dekker: New York, 1974.
3. Clark, A. H.; Richardson, R. K.; Ross-Murphy, S. B.; Stubbs, J. M. Macromolecules 1983, 16, 1367–1374.
4. McEvoy, H.; Ross-Murphy, S. B.; Clark, A. H. Polymer 1985, 26, 1493–1500.
5. Ziegler, G. R. Biohechnol Prog 1991, 7, 283–287.
6. Morris, E. R. Carbohydr Polym 1992, 17, 65–70.
7. Owen, A. J.; Jones, R. A. L. Macromolecules 1998, 31, 7336–7339.
8. Kolarik, J. Polym Compos 1997, 18, 433–441.
9. Davies, W. E. A. J Phys D Appl Phys 1971, 4, 1176–1181.
10. Kregers, A. F.; Teters, G. A. Mech Compos Mater 1979, 4, 377–383.
11. Kalidindi, S. R.; Franco, E. Compos Sci Technol 1997, 57, 293–305.
12. Kasapis, S.; Morris, E. R.; Norton, I. T.; Clark, A. H. Carbohydr Polym 1993, 21, 243–248.
13. Kasapis, S.; Morris, E. R.; Norton, I. T.; Gidley, M. J. Carbohydr Polym 1993, 21, 249–259.
14. Kasapis, S.; Morris, E. R.; Norton, I. T.; Brown, R. T. Carbohydr Polym 1993, 21, 261–268.
15. Kasapis, S.; Morris, E. R.; Norton, I. T.; Clark, A. H. Carbohydr Polym 1993, 21, 269–276.

16. Durrani, C. M.; Prystupa, D. A.; Donald, A. M.; Clark, A. H. Macromolecules 1993, 26, 981–987.
17. Durrani, C. M.; Donald, A. M. Macromolecules 1994, 27, 110–119.
18. Durrani, C. M.; Donald, A. M. Carbohydr Polym 1995, 28, 297–303.
19. Pudney, P. D. A.; Hancewicz, T. M. In 8th European Conference of Spectroscopy of Biological Molecules, in preparation.
20. Defloor, I.; Vandenreyken, V.; Grobet, P. J.; Delcour, J. A. J Chromatogr A 1998, 803, 103–109.
21. Normand, V.; Ravey, J. C. Rheol Acta 1997, 36, 610–617.
22. Turrell, G.; Corest, J. In Raman Microscopy Developments and Applications, Academic Press: New York, 1996.
23. Clark, A. H. In Food Polymers, Gels and Colloids; Dickinson, E., Ed.; Royal Society of Chemistry: London, 1991; p 322.
24. Meunier, V.; Nicolai, T.; Durand, D.; Parker, A. Macromolecules 1999, 32, 2610–2616.
25. Normand, V.; Muller, S.; Ravey, J. C.; Parker, A. Macromolecules 2000, 33, 1063–1071.
26. Andrew, J. J.; Hancewicz, T. M. Appl Spectrosc 1998, 52, 797–807.
27. Bohidar, H. B. Int J Biol Macromol 1998, 23, 1–6.